

# Spintronics meets nonadiabatic molecular dynamics: Geometric spin torque and damping on noncollinear classical magnetism due to electronic open quantum system

Utkarsh Bajpai and Branislav K. Nikolić

*Department of Physics and Astronomy, University of Delaware, Newark, DE 19716, USA*

We analyze quantum-classical hybrid system composed of two steadily precessing noncollinear slow classical localized magnetic moments embedded into an open quantum system of fast nonequilibrium conduction electrons. The electrons reside within a metallic wire connected to macroscopic reservoirs. The model captures the essence of realistic situations in spintronics involving dynamics of noncollinear magnetization configurations and textures, such as domain walls, skyrmions and spin waves. Its simplicity makes it possible to obtain the *exact* time-dependent nonequilibrium density matrix of electronic system and split it into four contributions. The Fermi surface contribution generates dissipative (or damping-like in spintronics terminology) spin torque on the moments, and one of the two Fermi sea contributions generates *geometric* torque dominating in the regime where electron spin is expected to adiabatically follow the instantaneous configuration of magnetic moments. When the coupling to the reservoirs is reduced, the geometric torque is the only nonzero contribution which can have both nondissipative (or field-like in spintronics) and dissipative components acting as the counterparts of geometric magnetism force and geometric friction in nonadiabatic molecular dynamics. Such *current-independent* geometric torque is *missing* from widely used micromagnetics or atomistic spin dynamics modeling of magnetization dynamics based on the Landau-Lifshitz-Gilbert (LLG) equation, and its form *cannot* be mimicked by simply renormalizing the LLG parameters.

One of the most fruitful applications of geometric (or Berry) phase [1] concepts is encountered in quantum-classical hybrid systems where separation of time scales makes it possible to consider fast quantum degrees of freedom interacting with the slow classical ones [2, 3]. The amply studied example of this kind are fast electrons interacting [4, 5] with slow nuclei in molecular dynamics (MD) [6, 7] where the parameters driving adiabatic evolution of quantum subsystem, with characteristic frequency smaller than its level spacing, are nuclear coordinates elevated to the status of dynamical variables. The electronic system then develops geometric phase in states evolving out of an instantaneous energy eigenstate, while also acquiring shifts in the energy levels. Conversely, nuclei experience forces due to back-action from electrons. The simplest force is the *adiabatic* Born-Oppenheimer (BO) force [4, 5] which depends only on the coordinates of the nuclei, and it is associated with electronic adiabatic potential surfaces [6, 7]. Even small violation of BO approximation leads to additional forces—the *first nonadiabatic* correction generates forces linear in the velocity of the nuclei, and being Lorentz-like they are dubbed [2, 8] “geometric magnetism.” The “magnetism” is not a not a real magnetic field, but an emergent geometrical property of the Hilbert space [9], and akin to the true Lorentz force, the emergent geometric force is *nondissipative*.

Additional forces emerge upon making the quantum system open by coupling it to a thermal bath [8, 10] (usually modeled as an infinite set of harmonic oscillators [11]) or to macroscopic reservoirs of particles [12]. In the latter case, one can also introduce chemical potential difference between the reservoirs to drive particle flux (i.e., current) through the quantum system which is, thereby, pushed out of equilibrium [12–15, 17]. In both

equilibrium and nonequilibrium cases, the energy spectrum of the quantum system is transformed into a continuous one, and geometric friction force [8, 12–17] linear in the velocity of the nuclei becomes possible. The friction is forbidden in the original analysis of Berry and Robbins [2] where the fast quantum system has discrete spectrum. Also, due to continuous spectrum, adiabaticity criterion has to be replaced by a different one, such as typical driving frequency should be smaller than the inverse dwell time of electrons within the active region [12]. Stochastic forces also appear, both in equilibrium and in nonequilibrium, where in the former case [8, 10] they are due to fluctuations at finite temperature while in the latter case they include additional contribution from nonequilibrium noise [12–14]. Finally, specific to nonequilibrium is the emergence of nonconservative forces [12–14, 17]. The derivation of these forces requires to analyze nonadiabatic corrections to the density matrix (DM) [8, 10, 12–15, 17]—this yields a non-Markovian stochastic Langevin equation, with nonlocal-in-time kernel describing memory effects [18], as the most general [14, 17] equation for nuclei in nonadiabatic MD.

The analogous quantum-classical problem exists in spintronics, where the fast quantum system are spins of conduction electron and slow system is comprised of localized-on-atoms classical spins and associated localized magnetic moments (LMMs) described by unit vectors  $\mathbf{M}_i(t)$ . The dynamics of LMMs is typically described by the Landau-Lifshitz-Gilbert (LLG) equation [19]

$$\frac{d\mathbf{M}_i}{dt} = -g\mathbf{M} \times \mathbf{B}_i^{\text{eff}} + \lambda\mathbf{M}_i \times \frac{d\mathbf{M}_i}{dt} + \frac{g}{\mu_M}(\mathbf{T}_i^{\text{DL}} + \mathbf{T}_i^{\text{FL}}). \quad (1)$$

This includes back-action of conduction electrons in the form of phenomenological Gilbert damping, whose parameter  $\lambda$  can be independently calculated [20] by using

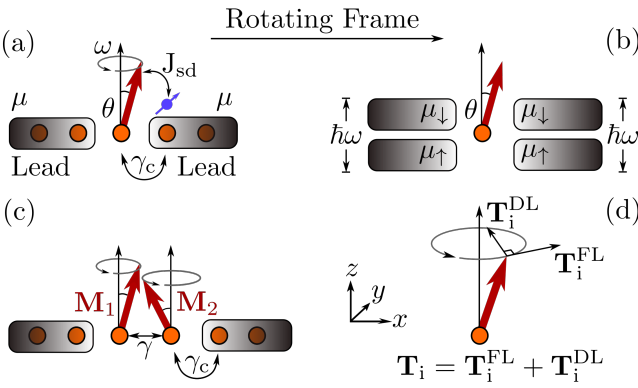


FIG. 1. (a) Schematic view of a two-terminal system where a single classical localized magnetic moment, precessing steadily with frequency  $\omega$  and cone angle  $\theta$ , interacts with open quantum system of conduction electron spins. The electrons hop along 1D infinite tight-binding chain which terminates into the left and right macroscopic reservoirs kept at the same chemical potential  $\mu$ . In panel (c), we consider two localized magnetic moments,  $\mathbf{M}_1$  and  $\mathbf{M}_2$ , which precess with the same frequency but are noncollinear due to  $\theta_1 \neq \theta_2$ . Both (a) and (c) can be mapped to a time-independent problem in the rotating frame where dc spin and charge currents are driven between four-terminals biased by voltage  $\hbar\omega$ . Panel (d) illustrates standard decomposition [Eq. (1)] of STT vector into FL and DL components, which are plotted in Figs. 2 and 3.

electronic Hamiltonian with spin-orbit coupling and impurities, as well as microscopically derived [21, 22] spin-transfer torque (STT),  $\mathbf{T}_i = \mathbf{T}_i^{\text{DL}} + \mathbf{T}_i^{\text{FL}}$ . The STT [23] requires electronic spin current as an input parameter. Semiclassical [21] or quantum transport [22] theory derivations, which traditionally also invoke phenomenological spin-flip relaxation time, do include *current-independent* nonadiabatic  $\propto \partial \mathbf{M}_i / \partial t$  back-action contributions to torque  $\mathbf{T}_i$ , but they are considered to be small and/or easily absorbable into Eq. (1) by simply renormalizing  $g$  and  $\lambda$  [21]. Here  $g$  is the gyromagnetic ratio;  $\mathbf{B}_i^{\text{eff}} = -\frac{1}{\mu_M} \partial \mathcal{H} / \partial \mathbf{M}_i$  is the effective magnetic field as the sum of external field, field due to interaction with other LMMs and magnetic anisotropy field; and  $\mu_M$  is the magnitude of LMM [19].

The STT [23] is phenomenon in which spin angular momentum of conduction electrons is transferred to local magnetization not aligned with electronic spin-polarization. As illustrated in Fig. 1(d), we perform the usual decomposition [23] of STT vector into: (i) even under time-reversal or field-like (FL) torque, which affects precession of LMM around  $\mathbf{B}_i^{\text{eff}}$ ; and (ii) odd under time-reversal or damping-like (DL) torque, which either enhances the Gilbert damping by pushing LMM toward  $\mathbf{B}_i^{\text{eff}}$  or competes with Gilbert term as “antidamping.” For example, negative values of  $T^{\text{DL}} = \mathbf{T}^{\text{DL}} \cdot \mathbf{e}_{\text{DL}}$  in Figs. 2 and 3, where  $\mathbf{e}_{\text{DL}} = (\mathbf{M}_i \times \partial \mathbf{M}_i / \partial t) |\mathbf{M}_i \times \partial \mathbf{M}_i / \partial t|^{-1}$ , means that  $\mathbf{T}^{\text{DL}}$  vector points away from the

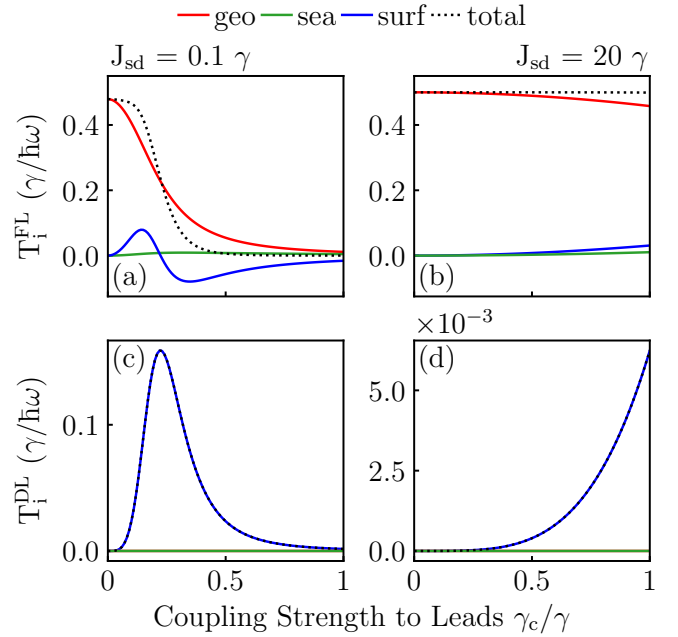


FIG. 2. The FL and DL components [Fig. (1)] of three spin torques in Eq. (5) exerted by nonequilibrium spin density of electrons onto a single localized precessing magnetic moment in the setup of Fig. 1(a) as a function of coupling to the leads. Black dotted line is the sum of the three torques. In panels (a) and (c)  $J_{sd} = 0.1$  eV, which corresponds to nonadiabatic regime, while in panels (b) and (d)  $J_{sd} = 20$  eV, which corresponds to perfectly adiabatic regime [27],  $J_{sd}/\hbar\omega \gg 1$ , for the chosen frequency of precession  $\hbar\omega = 0.001$  eV.

axis of precession which is antidamping action. Similarly,  $T^{\text{FL}} = \mathbf{T}^{\text{FL}} \cdot \mathbf{e}_{\text{FL}}$ , where  $\mathbf{e}_{\text{FL}} = (\partial \mathbf{M}_i / \partial t) |\partial \mathbf{M}_i / \partial t|^{-1}$ , is plotted in Figs. 2 and 3. The STT appears as the counterpart of nonconservative force in nonadiabatic MD, and Gilbert damping apparently looks like the counterpart of electronic friction [12–17] but it requires agents [20] other than electrons alone considered in nonadiabatic MD. Thus, the *geometric* torque and damping, as counterparts of geometric magnetism force and geometric friction [2, 8], are apparently *absent* from standard modeling of classical magnetization dynamics.

Geometric torque has been added *ad hoc* into the LLG equation applied to specific problems, such as spin waves within bulk magnetic materials [24–26]. A recent study [27] of a single classical LMM embedded into a closed (i.e., finite length one-dimensional wire) electronic quantum system finds that nonequilibrium electronic spin density always generates geometric torque, even in perfectly adiabatic regime where electron-spin/LMM interaction is orders of magnitude larger than the characteristic frequency of LMM dynamics. It acts as a purely FL torque causing anomalous frequency of precession that is higher than the Larmor frequency. By retracing the same steps [12, 13] in the derivation of the stochastic (Markovian) Langevin equation for electron-nuclei sys-

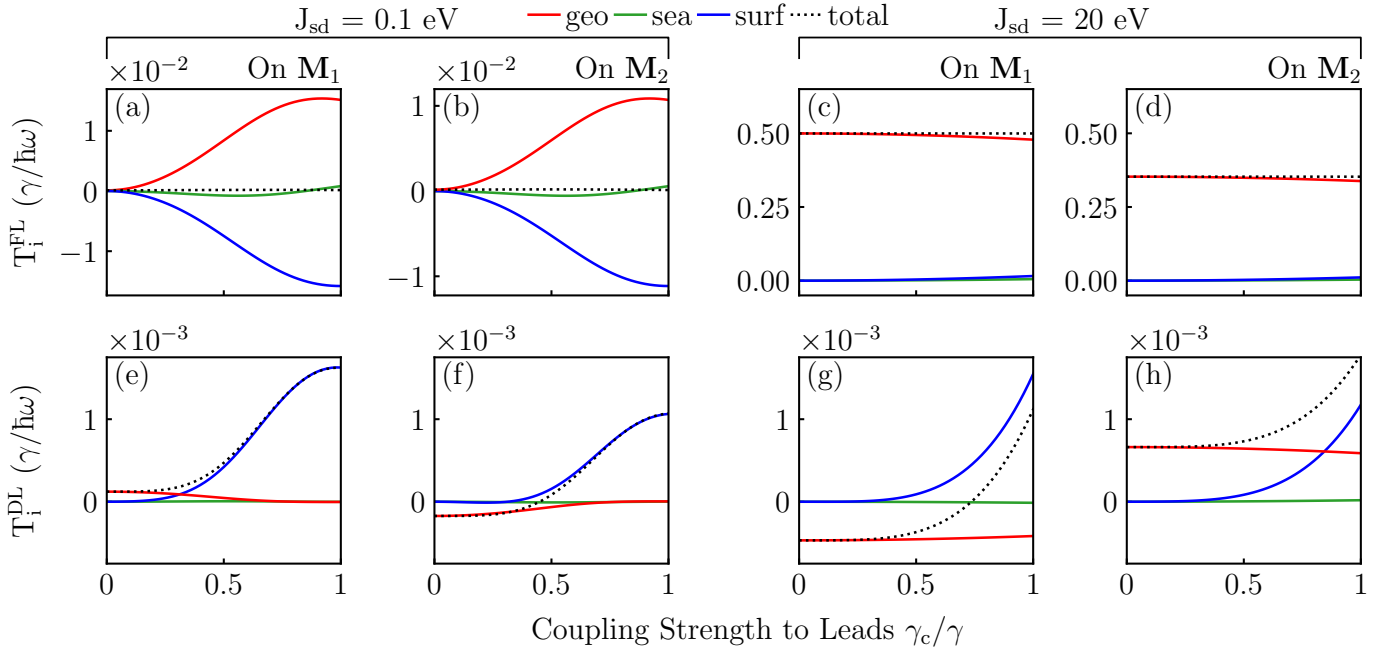


FIG. 3. The same information as in Fig. 2 but for spin torque components on two precessing localized magnetic moments  $\mathbf{M}_1$  and  $\mathbf{M}_2$  [Fig. 1(c)] as a function of coupling to the leads and for two different values of  $J_{sd}$ . The precession cone angle  $\theta_1 = 90^\circ$  and phase  $\phi_1 = 0^\circ$  are fixed for  $\mathbf{M}_1$ ; and  $\theta_2 = 45^\circ$  and  $\phi_2 = 90^\circ$  for  $\mathbf{M}_2$ .

tem connected to macroscopic reservoirs, Ref. [28] derived the stochastic LLG equation [29–31] for a single LMM embedded into an open electronic system out of equilibrium. The novelty in this derivation is geometric damping, present even in the absence of traditional spin-flip relaxation mechanisms [21, 22], while the same conclusion about geometric torque changing only the precession frequency of LMM has been reached (in some regimes, geometric phase can also affect the stochastic force [32]). However, single LMM is a rather special case (revisited in Fig. 2), and the most intriguing situations in spintronics involve dynamics of noncollinear textures of LMMs. This is exemplified by basic and applied research on current- or magnetic-field driven dynamics of domain walls and skyrmions [22, 33–35] where much richer panoply of back-action effects from fast electronic system can be expected.

In this Letter, we analyze an exactly solvable model of two steadily precessing LMMs,  $\mathbf{M}_1(t)$  and  $\mathbf{M}_2(t)$ , which are noncollinear and embedded into a one-dimensional (1D) infinite wire hosting conduction electrons, as illustrated in Fig. 1(c). Thus, the model can be viewed as a small segment of dynamical noncollinear magnetic texture or as two noncollinear macrospins of two coupled ferromagnetic layers (such as in the experiments on dynamic exchange coupling [36]). The choice of only two LMMs and 1D makes it exactly solvable—we compute the *exact time-dependent DM* via the nonequilibrium Green function (NEGF) formalism [37] for the setup in Fig. 1(c) and analyze different contributions to it in different regimes

of the ratio  $J_{sd}/\hbar\omega$  of *sd* exchange interaction  $J_{sd}$  [21] between electron spin and LMM and frequency of precession  $\omega$ . In both Figs. 1(a) and 1(c), the electronic subsystem is an *open quantum system* and, although no bias voltage is applied between the macroscopic reservoirs, it is pushed into the *nonequilibrium* by the dynamics of LMMs. For example, due to time-dependence of electronic quantum Hamiltonian generated by  $\mathbf{M}_1(t)$  [Fig. 1(a)] or  $\mathbf{M}_1(t)$  and  $\mathbf{M}_2(t)$  [Fig. 1(c)], spin current is pumped out of the active region into the leads [22, 38, 39]. Pumping of charge current will also occur if the left-right symmetry of the device is broken statically [38] or dynamically [40].

The conduction electron are modeled on an infinite 1D tight-binding (TB) clean chain with time-dependent Hamiltonian in the lab frame given by

$$\hat{H}_{\text{lab}}(t) = -\gamma \sum_i \hat{c}_i^\dagger \hat{c}_j - J_{sd} \sum_i \hat{c}_i^\dagger \hat{\sigma} \hat{c}_i \cdot \mathbf{M}_i(t). \quad (2)$$

Here  $\hat{c}_i^\dagger = (\hat{c}_{i\uparrow}^\dagger, \hat{c}_{i\downarrow}^\dagger)$  and  $\hat{c}_{i\sigma}^\dagger$  ( $\hat{c}_{i\sigma}$ ) creates (annihilates) an electron of spin  $\sigma = \uparrow, \downarrow$  at site  $i$ . The nearest-neighbor hopping  $\gamma = 1$  eV sets the unit of energy. The active region in Figs. 1(a) or 1(c) consists of one or two sites, respectively, while the rest of infinite TB chain is taken into account as the left (L) and the right (R) semi-infinite leads described by the same Hamiltonian in Eq. (2), but with  $J_{sd} = 0$ . The hopping between the leads and the active region is denoted as  $\gamma_c$  on the abscissa of Figs. 2 and 3. The leads terminate at infinity into the macroscopic particle reservoirs with identical chemical potentials  $\mu_L = \mu_R = E_F$  due to assumed absence of bias

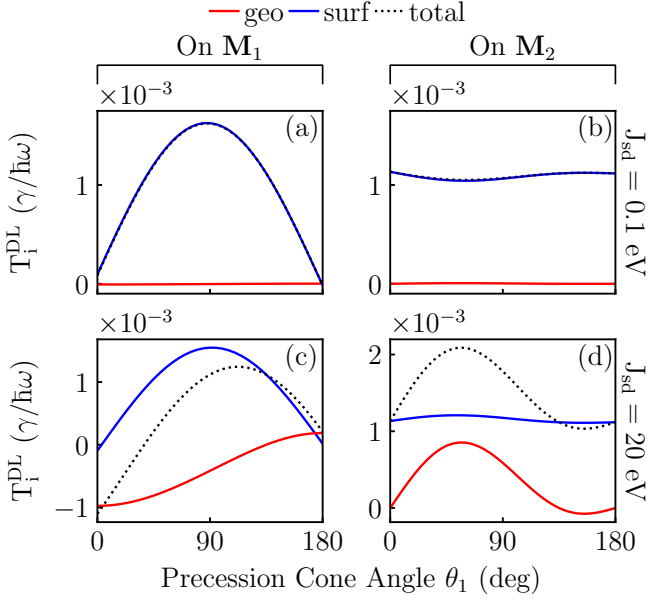


FIG. 4. The DL component of  $\mathbf{T}_i^{\text{geo}}$  and  $\mathbf{T}_i^{\text{surf}}$  spin torques in Eq. (5), as well as of their sum (black dotted line), on moments  $\mathbf{M}_1$  and  $\mathbf{M}_2$  in Fig. 1(c) as a function of the precession cone angle  $\theta_1$  while keeping  $\theta_2 = 45^\circ$  fixed. The phase angles are fixed as  $\phi_1 = 0^\circ$  for  $\mathbf{M}_1$  and  $\phi_2 = 90^\circ$  for  $\mathbf{M}_2$ , and  $\gamma_c/\gamma = 1$ .

voltage, and  $E_F = 0$  is chosen as the Fermi energy.

Instead of solving coupled LLG equations [Eq. (1)] for  $\mathbf{M}_1(t)$  and  $\mathbf{M}_2(t)$ , we impose a solution where both LMMs precess steadily around the  $z$ -axis in the counter-clockwise direction:  $M_i^x(t) = \sin \theta_i \cos(\omega t + \phi_i)$ ;  $M_i^y(t) = \sin \theta_i \sin(\omega t + \phi_i)$ ; and  $M_i^z(t) = \cos \theta_i$ . Using a unitary transformation into the rotating frame (RF), the Hamiltonian in Eq. (2) becomes time-independent [22, 38]

$$\hat{H}_{\text{RF}} = \hat{U}^\dagger(t) \hat{H}_{\text{lab}}(t) \hat{U}(t) - i\hbar \hat{U}^\dagger \frac{\partial \hat{U}}{\partial t} = \hat{H}_{\text{lab}}(t=0) - \frac{\hbar\omega}{2} \hat{\sigma}_z, \quad (3)$$

with magnetic moments frozen at  $t = 0$  configuration from the lab frame. The unitary operator is  $\hat{U}(t) = \exp(-i\omega t \hat{\sigma}_z/2)$ . In the RF, the original two-terminal Landauer setup for quantum transport in Figs. 1(a) and 1(c) is mapped, due to  $\hbar\omega\hat{\sigma}_z/2$  term in Eq. (3), onto an effective four-terminal Landauer setup [38] [illustrated for single LMM in Fig. 1(b)]. Each of its four leads is effectively half-metal ferromagnet which accepts only one spin species  $\uparrow$  or  $\downarrow$ , and there is dc bias voltage  $\hbar\omega/e$  between L or R pair of leads [Fig. 1(b)].

In the RF, the presence of the leads and macroscopic reservoirs can be taken into account exactly using steady-state NEGFs [37] which depend on time difference  $t - t'$  and energy  $E$  upon Fourier transform. Using the retarded Green function (GF),  $\hat{G}(E)$ , which gives density of states, and the lesser Green function  $\hat{G}^<(E)$ , which specifies how those states are occupied, we find the exact nonequilibrium DM of electrons in the RF

$\hat{\rho}_{\text{RF}} = \frac{1}{2\pi i} \int dE \hat{G}^<(E)$ . Here the two GFs are related by the Keldysh equation,  $\hat{G}^<(E) = \hat{G}(E)\hat{\Sigma}^<(E)\hat{G}^\dagger(E)$ , where  $\hat{\Sigma}^<(E)$  is the lesser self-energy [37] due to semi-infinite leads and  $\hat{G}(E) = [E - \hat{H}_{\text{RF}} - \hat{\Sigma}(E, \hbar\omega)]^{-1}$  with  $\hat{\Sigma}(E, \hbar\omega) = \sum_{p=\text{L,R}, \sigma=\uparrow, \downarrow} \Sigma_p^\sigma(E - Q_\alpha^\sigma \hbar\omega)$  being the sum of retarded self-energies for each of the four leads  $p$ ,  $\sigma$  in RF. We use shorthand notation  $Q_p^\uparrow = -1/2$  and  $Q_p^\downarrow = +1/2$ . Since typical frequency of magnetization dynamics is  $\hbar\omega \ll E_F$ , we can expand [41]  $\hat{\rho}_{\text{RF}}$  in small  $\hbar\omega/E_F$  and then transform it back to the lab frame,  $\hat{\rho}_{\text{lab}}(t) = \hat{U}(t)\hat{\rho}_{\text{RF}}\hat{U}^\dagger(t)$ . This yields four contributions to  $\hat{\rho}_{\text{lab}}(t) = \hat{\rho}_t^{\text{ad}} + \hat{\rho}_{\text{geo}}(t) + \hat{\rho}_{\text{sea}}(t) + \hat{\rho}_{\text{surf}}(t)$ :

$$\hat{\rho}_t^{\text{ad}} = -\frac{1}{\pi} \hat{U} \int_{-\infty}^{+\infty} dE \text{Im} \hat{G}_0 f(E) \hat{U}^\dagger, \quad (4a)$$

$$\hat{\rho}_{\text{geo}}(t) = \frac{1}{\pi} \hat{U} \int_{-\infty}^{+\infty} dE \text{Im} \left[ \hat{G}_0 \left( i\hbar \hat{U}^\dagger \frac{\partial \hat{U}}{\partial t} \right) \hat{G}_0 \right] f(E) \hat{U}^\dagger, \quad (4b)$$

$$\hat{\rho}_{\text{sea}}(t) = -\frac{\hbar\omega}{2\pi} \hat{U} \sum_p \int_{-\infty}^{+\infty} dE \text{Im} \left[ \hat{G}_0 \left( \frac{\partial \hat{\Sigma}_p^\uparrow}{\partial E} - \frac{\partial \hat{\Sigma}_p^\downarrow}{\partial E} \right) \hat{G}_0 \right] \times f(E) \hat{U}^\dagger, \quad (4c)$$

$$\hat{\rho}_{\text{surf}}(t) = \frac{\hbar\omega}{4\pi} \hat{U} \sum_p \int_{-\infty}^{+\infty} dE \hat{G}_0 (\hat{\Gamma}_p^\uparrow - \hat{\Gamma}_p^\downarrow) \hat{G}_0^\dagger \frac{\partial f}{\partial E} \hat{U}^\dagger. \quad (4d)$$

We confirm by numerically exact calculations [33] that thus obtained  $\hat{\rho}_{\text{lab}}(t)$  is identical to  $G^<(t, t)/i$  computed directly in the lab frame. Here  $\hat{G}_0(E) = [E - \hat{H}_{\text{RF}} - \hat{\Sigma}(E, 0)]^{-1}$  is obtained from  $\hat{G}(E)$  by setting  $\hbar\omega = 0$ ;  $\hat{\Gamma}_p^\sigma(E) = i[\hat{\Sigma}_p^\sigma(E) - \hat{\Sigma}_p^\sigma(E)^\dagger]$  is the level broadening matrix due to coupling to the leads; and  $f_p^\sigma(E) = f(E - [E_F + Q_\alpha^\sigma \hbar\omega])$  is the Fermi function of macroscopic reservoir  $p$ ,  $\sigma$  in the RF.

The trace  $\langle \hat{\mathbf{s}}_i \rangle(t) = \text{Tr}[\hat{\rho}_{\text{lab}}(t)|i\rangle\langle i| \otimes \hat{\sigma}]$  gives total electronic spin density with four contributions whose time-dependence is animated in two movies provided as the Supplemental Material [43]. The contribution  $\langle \hat{\mathbf{s}}_i \rangle_t^{\text{ad}}$  is the equilibrium expectation value at an instantaneous time  $t$  which defines ‘adiabatic spin density’ [21, 22, 25–27]. It is computed using  $\hat{\rho}_t^{\text{ad}}$  as the grand canonical equilibrium DM expressed using frozen (adiabatic) retarded Green function [12, 13, 28],  $\hat{G}_t(E) = [E - \hat{H}_t - \hat{\Sigma}]^{-1}$ , for instantaneous configuration of  $\mathbf{M}_i(t)$  while assuming  $d\mathbf{M}_i/dt = 0$  [subscript  $t$  signifies parametric dependence on time through slow variation of  $\mathbf{M}_i(t)$ ]. The other three contributions—from  $\hat{\rho}_{\text{geo}}(t)$  and  $\hat{\rho}_{\text{sea}}(t)$  governed by the Fermi sea and  $\hat{\rho}_{\text{surf}}(t)$  governed by the Fermi surface electronic states—contain first nonadiabatic correction [12, 13, 28] proportional to velocity  $d\mathbf{M}_i/dt$ , as well as higher order terms due to  $\hat{\rho}_{\text{lab}}(t)$  being exact. These three define STT out of equilibrium [21, 33, 41]

$$\mathbf{T}_i = J_{sd} \langle \hat{\mathbf{s}}_i(t) \rangle \times \mathbf{M}_i(t) = \mathbf{T}_i^{\text{geo}} + \mathbf{T}_i^{\text{sea}} + \mathbf{T}_i^{\text{surf}}, \quad (5)$$

where each term  $\mathbf{T}_i^{\text{geo}}$ ,  $\mathbf{T}_i^{\text{sea}}$ ,  $\mathbf{T}_i^{\text{surf}}$  can be additionally separated into its own DL and FL components [Eq. (1)], as plotted in Figs. 2 and 3. Note that  $\mathbf{T}_i^{\text{sea}}$  is insignificant in both Figs. 2 and 3, so we focus on  $\mathbf{T}_i^{\text{geo}}$  and  $\mathbf{T}_i^{\text{surf}}$ .

To gain transparent physical interpretation of  $\mathbf{T}_i^{\text{geo}}$  and  $\mathbf{T}_i^{\text{surf}}$ , we first consider the simplest case [27, 28]—a single  $\mathbf{M}_1(t)$  in setup of Fig. 1(a). The STT contributions as a function of the coupling  $\gamma_c$  to the leads (i.e., reservoirs) are shown in Fig. 2. We use two different values for  $J_{sd}$ , where large ratio of  $J_{sd} = 20$  eV and  $\hbar\omega = 0.001$  eV is perfect adiabatic limit [25–27]. Nevertheless, even in this limit and for  $\gamma_c \rightarrow 0$  we find  $\mathbf{T}_1^{\text{geo}} \neq 0$  in Fig. 1(c) as the only nonzero and *purely* FL torque. This is also found in closed system of Ref. [27] where  $\mathbf{T}_1^{\text{geo}}$  was expressed in terms of the spin Berry curvature. As the quantum system becomes opened for  $\gamma_c > 0$ ,  $\mathbf{T}_1^{\text{geo}}$  is slightly reduced while  $\mathbf{T}_1^{\text{surf}}$  emerges with small FL [Fig. 2(b)] and large DL [Fig. 2(d)] components. The DL torque points toward the  $z$ -axis and, therefore, enhances the Gilbert damping. In the wide-band limit, the self-energy  $\hat{\Sigma}(E) = -i\Gamma\hat{I}_2$  is energy-independent, which makes it possible to obtain analytical expression for  $\mathbf{T}_1^{\text{geo}}(t)$  at zero temperature

$$\mathbf{T}_1^{\text{geo}}(t) = \frac{\hbar\omega}{2\pi} \left[ \pi - 2 \tan^{-1} \left( \frac{\Gamma}{J_{sd}} \right) \right] \sin \theta \mathbf{e}_\phi(t), \quad (6)$$

where  $\mathbf{e}_\phi(t) = -\sin \omega t \mathbf{e}_x + \cos \omega t \mathbf{e}_y$ . Thus, in perfect adiabatic limit,  $J_{sd}/\hbar\omega \rightarrow \infty$ , or in closed system,  $\Gamma \rightarrow 0$ ,  $\mathbf{T}_1^{\text{geo}}$  is independent of microscopic parameters as expected from its geometric nature [24]. The always present  $\mathbf{T}_i^{\text{geo}} \neq 0$  means that electron spin is *never* along ‘adiabatic direction’  $\langle \hat{s}_i \rangle_t^{\text{ad}}$ . This can also be contrasted with electron-nuclei systems where geometric force sometimes appears as an artifact of the BO approximation [4, 5].

As we add second  $\mathbf{M}_2(t)$  in Fig. 3,  $\mathbf{T}_i^{\text{geo}}$  acquires DL component, even in closed system  $\gamma_c \rightarrow 0$ , which can have both damping [Fig. 3(e),(h)] and antidamping [Fig. 3(f),(g)] action. Interestingly,  $\mathbf{T}_i^{\text{geo,FL}} + \mathbf{T}_i^{\text{sea,FL}} + \mathbf{T}_i^{\text{surf,FL}} \equiv 0$  on both LMMs in Fig. 3(a),(b). The total DL torque in Fig. 3(e)–(h),  $\mathbf{T}_i^{\text{DL}} = \mathbf{T}_i^{\text{geo,DL}} + \mathbf{T}_i^{\text{surf,DL}}$ , can be viewed as the consequence of time-retardation effects [34, 42], where in the perturbative limit of small  $J_{sd}$  and small  $\Gamma$  electrons can be ‘integrated out’ [21, 29–31] to cast [34] DL torque as  $|\mathbf{T}_i^{\text{DL}}(t)| = \lambda(t)|\mathbf{M}_i \times \partial\mathbf{M}_i/\partial t| = \omega\lambda_i(t)\sin\theta_i(t)$ . Thus, to examine whether such DL torque could be included into the LLG equation of micromagnetics and atomistic spin dynamics [19] by a simple renormalization [21] of the LLG parameters [Eq. (1)], one needs to confirm that  $\lambda_i(t)$  is time-independent constant. Although  $|\mathbf{T}_1^{\text{DL}}(t)| \propto \sin\theta_1$  is approximately satisfied in Fig. 4(a), meaning that  $\lambda_1 \approx \text{cons.}$ ,  $|\mathbf{T}_i^{\text{DL}}(t)| \not\propto \sin\theta_1$  in all other cases in Fig. 4(c)–(d) indicating that effective  $\lambda_i(t)$  is time-dependent. This suggests that geometric and Fermi surface torques, which are *current-independent*, should be included by self-consistent coupling of electronic DM

and LLG equation calculations, as proposed in Refs. [33–35, 42] and in analogy to how electronic friction is included in nonadiabatic MD [7, 12–17].

This work was supported by NSF Grant No. CHE 1566074.

---

- [1] M. V. Berry, Quantal phase factors accompanying adiabatic changes, Proc. R. Soc. Lond. A **392**, 45 (1984).
- [2] M. V. Berry and J. M. Robbins, Chaotic classical and half-classical adiabatic reactions: geometric magnetism and deterministic friction, Proc. R. Soc. Lond. A **442**, 659 (1993).
- [3] Q. Zhang and B. Wu, General approach to quantum-classical hybrid systems and geometric forces, Phys. Rev. Lett. **97**, 190401 (2006).
- [4] S. K. Min, A. Abedi, K. S. Kim, and E. K. U. Gross, Is the molecular Berry phase an artifact of the Born-Oppenheimer approximation?, Phys. Rev. Lett. **113**, 263004 (2014).
- [5] R. Requist, F. Tandetzky, and E. K. U. Gross, Molecular geometric phase from the exact electron-nuclear factorization, Phys. Rev. A **93**, 042108 (2016).
- [6] I. G. Ryabinkin, L. Joubert-Doriol, and A. F. Izmaylov, Geometric phase effects in nonadiabatic dynamics near conical intersections, Acc. Chem. Res. **50**, 1785 (2017).
- [7] W. Dou and J. E. Subotnik, Nonadiabatic molecular dynamics at metal surfaces, J. Phys. Chem. A **124**, 757 (2020).
- [8] M. Campisi, S. Denisov, and P. Hänggi, Geometric magnetism in open quantum systems, Phys. Rev. A **86**, 032114 (2012).
- [9] M. Kolodrubetz, D. Sels, P. Mehta, and A. Polkovnikov, Geometry and non-adiabatic response in quantum and classical systems, Phys. Rep. **697**, 1 (2017).
- [10] F. Gaitan, Berry’s phase in the presence of a stochastically evolving environment: A geometric mechanism for energy-level broadening, Phys. Rev. A **58**, 1665 (1998).
- [11] R. S. Whitney and Y. Gefen, Berry phase in a nonisolated system, Phys. Rev. Lett. **90**, 190402 (2003).
- [12] M. Thomas, T. Karzig, S. V. Kusminskiy, G. Zaránd, and F. von Oppen, Scattering theory of adiabatic reaction forces due to out-of-equilibrium quantum environments, Phys. Rev. B **86**, 195419 (2012).
- [13] N. Bode, S. V. Kusminskiy, R. Egger, and F. von Oppen, Scattering theory of current-induced forces in mesoscopic systems, Phys. Rev. Lett. **107**, 036804 (2011).
- [14] J.-T. Lü, M. Brandbyge, P. Hedegård, T. N. Todorov, and D. Dundas, Current-induced atomic dynamics, instabilities, and Raman signals: Quasiclassical Langevin equation approach, Phys. Rev. B **85**, 245444 (2012).
- [15] W. Dou, G. Miao, and J. E. Subotnik, Born-Oppenheimer dynamics, electronic friction, and the inclusion of electron-electron interactions, Phys. Rev. Lett. **119**, 046001 (2017).
- [16] W. Dou and J. E. Subotnik, Perspective: How to understand electronic friction, J. Chem. Phys. **148**, 230901 (2018).
- [17] F. Chen, K. Miwa, and M. Galperin, Current-induced forces for nonadiabatic molecular dynamics, J. Phys. Chem. A **123**, 693 (2019).

[18] R. L. S. Farias, R. O. Ramos, and L. A. da Silva, Stochastic Langevin equations: Markovian and non-Markovian dynamics, *Phys. Rev. E* **80**, 031143 (2009).

[19] R. F. L. Evans, W. J. Fan, P. Chureemart, T. A. Ostler, M. O. A. Ellis, and R. W. Chantrell, Atomistic spin model simulations of magnetic nanomaterials, *J. Phys.: Condens. Matter* **26**, 103202 (2014).

[20] A. A. Starikov, P. J. Kelly, A. Brataas, Y. Tserkovnyak, and G. E. W. Bauer, Unified first-principles study of Gilbert damping, spin-flip diffusion, and resistivity in transition metal alloys, *Phys. Rev. Lett.* **105**, 236601 (2010).

[21] S. Zhang and Z. Li, Roles of nonequilibrium conduction electrons on the magnetization dynamics of ferromagnets, *Phys. Rev. Lett.* **93**, 127204 (2004).

[22] G. Tatara, Effective gauge field theory of spintronics, *Physica E* **106**, 208 (2019).

[23] D. Ralph and M. Stiles, Spin transfer torques, *J. Magn. Mater.* **320**, 1190 (2008).

[24] X. G. Wen and A. Zee, Spin waves and topological terms in the mean-field theory of two-dimensional ferromagnets and antiferromagnets, *Phys. Rev. Lett.* **61**, 1025 (1988).

[25] Q. Niu and L. Kleinman, Spin-wave dynamics in real crystals, *Phys. Rev. Lett.* **80**, 2205 (1998).

[26] Q. Niu, X. Wang, L. Kleinman, W.-M. Liu, D. M. C. Nicholson, and G. M. Stocks, Adiabatic dynamics of local spin moments in itinerant magnets, *Phys. Rev. Lett.* **83**, 207 (1999).

[27] C. Stahl and M. Potthoff, Anomalous spin precession under a geometrical torque, *Phys. Rev. Lett.* **119**, 227203 (2017).

[28] N. Bode, L. Arrachea, G. S. Lozano, T. S. Nunner and F. von Oppen, Current-induced switching in transport through anisotropic magnetic molecules, *Phys. Rev. B* **85**, 115440 (2012).

[29] M. Onoda and N. Nagaosa, Dynamics of localized spins coupled to the conduction electrons with charge and spin currents, *Phys. Rev. Lett.* **96**, 066603 (2006).

[30] A. S. Núñez and R. A. Duine, Effective temperature and Gilbert damping of a current-driven localized spin, *Phys. Rev. B* **77**, 054401 (2008).

[31] J. Fransson and J.-X. Zhu, Spin dynamics in a tunnel junction between ferromagnets, *New J. Phys.* **10**, 013017 (2008).

[32] A. Shnirman, Y. Gefen, A. Saha, I. S. Burmistrov, M. N. Kiselev, and A. Altland, Geometric quantum noise of spin, *Phys. Rev. Lett.* **114**, 176806 (2015).

[33] M. D. Petrović, B. S. Popescu, U. Bajpai, P. Plecháč, and B. K. Nikolić, Spin and charge pumping by a steady or pulse-current-driven magnetic domain wall: A self-consistent multiscale time-dependent quantum-classical hybrid approach, *Phys. Rev. Applied* **10**, 054038 (2018).

[34] U. Bajpai and B. K. Nikolić, Time-retarded damping and magnetic inertia in the Landau-Lifshitz-Gilbert equation self-consistently coupled to electronic time-dependent nonequilibrium Green functions, *Phys. Rev. B* **99**, 134409 (2019).

[35] M. D. Petrović, P. Plecháč, and B. K. Nikolić, Annihilation of topological solitons in magnetism: How domain walls collide and vanish to burst spin waves and pump electronic spin current of broadband frequencies, [arXiv:1908.03194](https://arxiv.org/abs/1908.03194) (2019).

[36] B. Heinrich, Y. Tserkovnyak, G. Woltersdorf, A. Brataas, R. Urban, and G. E. W. Bauer, Dynamic exchange coupling in magnetic bilayers, *Phys. Rev. Lett.* **90**, 187601 (2003).

[37] G. Stefanucci and R. van Leeuwen, *Nonequilibrium Many-Body Theory of Quantum Systems: A Modern Introduction* (Cambridge University Press, Cambridge, 2013).

[38] S.-H Chen, C.-R Chang, J. Q. Xiao and B. K. Nikolić, Spin and charge pumping in magnetic tunnel junctions with precessing magnetization: A nonequilibrium Green function approach, *Phys. Rev. B* **79**, 054424 (2009).

[39] Y. Tserkovnyak, A. Brataas, G. E. W. Bauer, and B. I. Halperin, Nonlocal magnetization dynamics in ferromagnetic heterostructures, *Rev. Mod. Phys.* **77**, 1375 (2005).

[40] U. Bajpai, B. S. Popescu, P. Plecháč, B. K. Nikolić, L. E. F. Foa Torres, H. Ishizuka, and N. Nagaosa, Spatio-temporal dynamics of shift current quantum pumping by femtosecond light pulse, *J. Phys.: Mater.* **2**, 025004 (2019).

[41] F. Mahfouzi and B. K. Nikolić, How to construct the proper gauge-invariant density matrix in steady-state nonequilibrium: Applications to spin-transfer and spin-orbit torque, *SPIN* **03**, 02 (2013).

[42] M. Sayad and M. Potthoff, Spin dynamics and relaxation in the classical-spin Kondo-impurity model beyond the Landau-Lifshitz-Gilbert equation, *New J. Phys.* **17**, 113058 (2015).

[43] See Supplemental Material at <https://wiki.physics.udel.edu/qttg/Publications> for two movies which animate time evolution of three contributions to electronic spin density— $\langle \hat{s}_i \rangle_t^{\text{ad}}$  (orange arrow),  $\langle \hat{s}_i \rangle_t^{\text{geo}}(t)$  (red arrow) and  $\langle \hat{s}_i \rangle_t^{\text{surf}}(t)$  (blue arrow)—due to a single [Fig. 1(a)] or two [Fig. 1(c)] steadily precessing LMMs embedded into electronic open quantum system with  $\gamma_c/\gamma = 1$  coupling strength to the leads. The length of the arrows corresponds to the magnitude of these vectors which are used in Figs. 2 and 3 to compute the corresponding STT via Eq. (5). Note that in the case of single LMM for both values of  $J_{sd}$ , or for two LMMs using  $J_{sd} = 20$  eV,  $\langle \hat{s}_i \rangle_t^{\text{ad}}$  is parallel to  $\mathbf{M}_i(t)$  so that orange and black arrows overlap [i.e., one sees orange dots along the black arrow representing  $\mathbf{M}_i(t)$  in the movies].